Received: 17 August 2025 | Revised: 9 November 2025 | Accepted: 4 January 2026 | Published online: 13 January 2026

RESEARCH ARTICLE

Medinformatics
2026, Vol. 00(00) 1–14
DOI: 10.47852/bonviewMEDIN62027245

BON VIEW PUBLISHING

MOMMI-MP: A Comprehensive Database for Integrated Analysis of Metabolic and Microbiome Profiling of Mouse Pregnancy

Kaustubh K. Pachpor[1, †], Julianne Jorgensen[1, 2, †], Medha Priyadarshini[2], Derek J. Reiman[3], Brian T. Layden[2, 4] and Yang Dai[1, 5,*]

[1] *Department of Biomedical Engineering, University of Illinois Chicago, USA*

[2] *Division of Endocrinology, Diabetes, and Metabolism, University of Illinois Chicago, USA*

[3] *Toyota Technological Institute at Chicago, USA*

[4] *Jesse Brown Veterans Affair Medical Center, USA*

[5] *Center for Bioinformatics and Quantitative Biology, University of Illinois Chicago, USA*

Abstract: Pregnancy is a dynamic physiological state characterized by extensive metabolic changes. The development of insulin resistance later in gestation is a normal adaptation that supports fetal growth and a physiological response in pregnancy. However, if metabolic aberrations occur above the normal insulin resistance, gestational diabetes mellitus, a form of diabetes that appears during pregnancy, can develop. Multi-omics approaches are powerful tools to uncover the mechanisms that drive metabolic changes in different physiological and pathological states. A recent multi-omics mouse study collected pregnancy-specific physiological and metabolic profiles, 16S rRNA microbiome, and plasma untargeted LC-MS metabolome data from 3 genetically diverse strains of mice (C57BL/6J, CD1, and NIH-Swiss) over 6 timepoints: gestational days 0, 10, 15, and 19, and postpartum days 3 and 20, totaling 60 samples for each strain. To facilitate the utilization of these impactful data by other researchers, we developed Multi-omics Metabolic & Microbiome Profiling of Mouse Pregnancy (MOMMI-MP), a database that provides an easy-to-use platform to browse and search differentially abundant microbial taxa, metabolites, metabolic pathways, and predicted micro-metabolite interactions using an array of state-of-the-art statistical and machine learning models. Our analysis revealed a previously unrecognized gut microbial–host metabolic pathway involving indoleamine 2,3-dioxygenase 1 (IDO1) and kynurenine, which plays a crucial role in mediating pregnancy-related metabolic adaptations, as well as other significant microbiome and metabolic changes. The computational results are presented in various tables and plots, organized in MOMMI-MP, to empower exploratory analyses by other researchers. Representing a significant new resource, MOMMI-MP provides a tool for researchers to facilitate the investigation of novel mechanisms governing metabolic changes during pregnancy.

Keywords: gestational diabetes mellitus, insulin resistance, microbiome, metabolome

1. Introduction

Gestational diabetes mellitus (GDM) is a prevalent metabolic disorder during pregnancy, affecting approximately 5–9% of pregnancies annually in the United States, with incidence increasing with maternal age [1, 2]. Notably, up to 60% of women with GDM have an increased risk of developing type 2 diabetes later in life [3]. GDM is characterized by impaired glucose tolerance and insulin resistance, resulting in reduced glucose uptake and utilization [4]. Interestingly, a certain degree of insulin resistance is a normal physiological adaptation in later stages of pregnancy [5, 6]. Recent studies have shown that altered metabolic profiles during pregnancy are associated with compositional changes in the gut microbiome [7]. During pregnancy, hormone levels, along with other host factors, influence the gut microbiome [6]. In the third trimester, these microbiome changes are associated with increased inflammatory markers resembling dysbiosis found in metabolic syndrome [6]. Studying the multifactorial nature of gut microbiome and metabolomics and their contribution to the development of insulin resistance in normal pregnancy is important to elucidate a clearer understanding of the mechanism and development of GDM.

*Corresponding author: Yang Dai, Department of Biomedical Engineering, University of Illinois Chicago, and Center for Bioinformatics and Quantitative Biology, University of Illinois Chicago, USA. Email: yangdai@uic.edu

To investigate these multifactorial changes, we employed a systems biology approach to collect metabolic health, gut microbial, and metabolomic profiles from three genetically diverse mouse strains (C57BL/6J, CD1, and NIH-Swiss) during both the gestational and postpartum periods. The data analysis uncovered a previously unknown gut microbial–host metabolic pathway, including indoleamine-2,3 dioxygenase 1 and kynurenine, which is crucial in mediating pregnancy-related metabolic adaptations [5]. This multi-omics study provided a wealth of information encompassing pregnancy-specific physiological and metabolic responses, the composition of the gut microbiome, and the plasma metabolome generated from 6 timepoints—gestational days 0, 10, 15, and 19 and postpartum days 3 and 20—totaling 60 samples for each mouse strain. Given the complex nature of insulin resistance in normal pregnancy, the datasets obtained from this highly controlled study hold immense potential to yield valuable insights into the intricate interactions between metabolic responses, gut microbes, and the specific metabolites that mediate these effects. However, reanalyzing the publicly available multi-omics data presents significant challenges for individuals who need more bioinformatics expertise.

Our study aims, therefore, are designed to address these needs by developing MOMMI-MP (Multi-omics Metabolic & Microbiome Profiling of Mouse Pregnancy), ensuring the database is user-friendly and highly accessible to facilitate the investigation of microbiome and metabolic alterations during pregnancy. This comprehensive database offers results from the in-depth analysis of the data for each mouse strain across gestation and postpartum time points, including strain-specific (1) differentially abundant (DA) microbial taxa and metabolites, as well as the metabolic pathways enriched for these metabolites, (2) microbes and metabolites significantly correlated with metabolic health characteristics, and (3) significantly correlated microbe and metabolite pairs. The database also contains a list of metabolites whose abundance is predicted from significant microbial abundances, a microbe–metabolite module interaction network, and a detailed list of involved microbes and metabolites with their significant statistical interactions in all strains predicted using MiMeNet, a neural network model [8]. The results included in MOMMI-MP were generated using uniform preprocessing procedures and the most reputable bioinformatic and statistical analysis tools (Figure 1). With access to the information in MOMMI-MP (https://mommi-mp.github.io/Plots/), researchers from diverse scientific backgrounds can easily access and harness the power of this resource to advance their investigations in related research areas.

2. Methods and Materials

2.1. Datasets and preprocessing

The published multi-omics datasets consist of mouse metabolic health characteristics, microbiome, and metabolomic profiles measured at 4 time points during gestation (day 0, 10, 15, and 19) and 2 time points postpartum (PP3, and PP20) from 3 mouse strains, C57BL/6J (Jackson Laboratory), CD-1 (Charles River Labs), and NIH-Swiss (Envigo), with 10 mice at each time point per strain starting at 10 weeks old [5]. Pregnancy in female C57 (Jackson Laboratory), CD-1 (Charles River Labs), and NIH-Swiss mice with strain-specific males was confirmed, and samples were collected and stored at −80 °C [5]. The metabolic health characteristics comprise blood glucose and insulin levels, body weight,

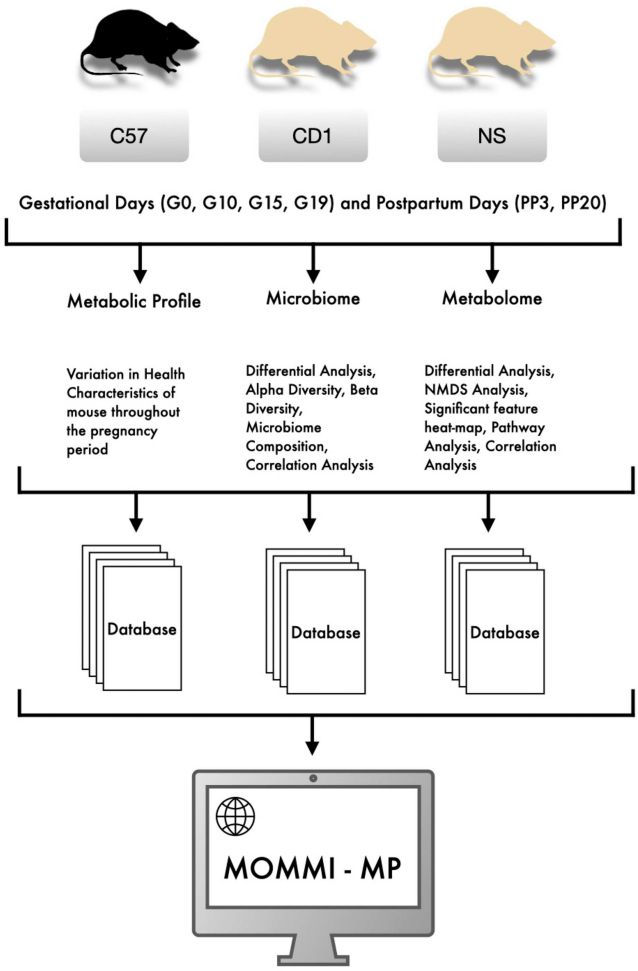

Figure 1 The structural outline of MOMMI-MP

and changes in the weights of different adipose depots (subcutaneous and visceral) at each pregnancy time point. The detailed experimental protocols for data collection and quantification procedures for microbiome and metabolomic features can be found in the earlier publication [5].

2.2. Untargeted LC-MS/MS metabolomics

Plasma at each timepoint was assayed for untargeted metabolomics via liquid chromatography with tandem mass spectroscopy (LC-MS/MS) (Agilent 1290 Infinity LC System coupled to an Agilent 6545 Accurate mass quadrupole time-of-flight (Q-TOF) with a dual Agilent Jet Stream source) [5, 9]. Additional details are in the supplementary methods section.

2.3. Microbiome 16S rRNA sequencing

To generate the microbiome profiles, the bacterial 16S rRNA was extracted from stool samples, and the V4 region (515F-806R) was amplified and sequenced on the Illumina MiSeq (Argonne National Laboratory Core) following standard protocols from the Earth Microbiome Project (earthmicrobiome.org/emp-standard-protocols/its/). Additional details are in the supplementary methods section.

2.4. Alpha diversity and beta diversity of microbiomes

Alpha diversity was obtained by rarifying the dataset by the even depth method and functions such as "ggplot," "plot_richness," and "estimate richness" in the Phyloseq package [13]. The "Strain" attribute of the dataset was used to perform the analysis. Two methods, "Observed" and "Shannon," were used to display the results of the same. The dataset was rarefied, and the Binary Jaccard metric was used to perform the Non-metric Multidimensional Scaling (NMDS) analysis using the "metaMDS" function from the "vegan" library [14], whereas the Bray–Curtis distance was used in principal coordinate analysis (PCoA).

2.5. Differential analysis of microbiome data

This analysis aimed to identify taxa (microbial features) whose absolute abundances differed significantly at different time points during pregnancy compared to the starting point "G0" (Gestation Day 0). Analysis of Composition of Microbiomes with Bias Correction (ANCOM-BC) [15] was chosen over multiple available tools because it is specifically designed to handle compositional data and can correct the bias induced by the differences among samples. In our analysis, the data over the pregnancy period were imported at once into the Bioconductor package "ANCOM-BC." The time points were defined by the "Day" factor, with G0 as the reference point. By comparing each time point individually to the reference point G0, the analysis detects microbial taxa that are DA at G10, G15, and G19 during gestation and at PP3 and PP20 during postpartum, compared to day G0, respectively. The results were summarized in a table with the names of the DA microbes and the adjusted *p*-values using a threshold of α=0.05 for controlling false discovery rate (FDR). The differential analysis was performed at each taxonomic level except "Kingdom" and "Phylum" for each strain.

2.6. Differential analysis of metabolomes

PERMANOVA [16] analysis was performed on two groups of samples: one group comprised samples collected at gestational time points G15 and G19, and the other group consisted of samples from all the remaining time points. This grouping was determined based on the previous results that indicated distinguishable metabolomic profiles at G15 and G19 compared to the other time points [5]. PERMANOVA assesses the statistical significance of separating these two groups by evaluating the overall dissimilarity or distance between the samples within and between the groups. It uses a permutation-based procedure to generate a distribution of possible test statistic values under the null hypothesis of no group differences. By comparing the observed test statistic to the null distribution, an empirical *p*-value can be obtained. The PERMANOVA analysis results in a list of DA metabolite features and their adjusted *p*-values between the two groups. These metabolite features are potentially associated with pregnancy-induced insulin resistance, as G15 and G19 are considered the period when peak insulin resistance is observed. The threshold of 0.05 was applied to the adjusted *p*-values for controlling FDR.

2.7. Mapping metabolite features to annotated compounds

The Mummichog algorithm implemented in the online tool MetaboAnalyst [17] was used to identify the KEGG pathways and the compound hits from the DA metabolite features identified from the differential analysis. Mummichog takes advantage of the organization of metabolic networks to predict functional activity directly from metabolite feature tables, circumventing ambiguity in metabolite identification. The input to Mummichog was the table of DA metabolite features and their adjusted *p*-values obtained from the PERMANOVA analysis. The parameters used were as follows: mass tolerance was set to 10 ppm, and retention time was set to "seconds." The tool's output includes a visual representation of the pathways and multiple tables, which give the mapped compound IDs and significant hits for every pathway. The compound IDs and the adjusted *p*-value table were used in KEGG-Rest [18] to identify the compound names, which were later used to replace the unique metabolite feature ID and filter out the significant features that are not linked to any compounds. The abundance table of the mapped DA metabolites was then used to perform correlation analysis with the identified DA microbes.

2.8. Correlation analysis

Three types of correlation analysis were performed: (1) the DA microbes identified using ANCOM-BC and the metabolic health characteristics of the mice, (2) the DA metabolites and the metabolic health characteristics, and (3) the DA metabolites and DA microbes. Pearson's correlations were calculated. The analysis was performed at each taxonomic level for each strain.

2.9. Pathway analysis

The Mummichog algorithm in MetaboAnalyst [17] leverages the power of statistical enrichment analysis to determine whether certain pathways were overrepresented by the annotated compounds. The significance of pathways is indicated by the gamma value, representing the adjusted *p*-values obtained from the enrichment analysis. The *p*-value table of all metabolite features obtained from the PERMANOVA analysis was used as the input to the Mummichog algorithm (with a threshold of 0.05). The Mus musculus (mouse) KEGG pathway library was used to map the pathways. The resulting table contains the enriched pathways along with their respective gamma values.

2.10. Integrative analysis of microbiomes and metabolomes using MiMeNet

MiMeNet is a powerful neural network framework to uncover the intricate interactions between the gut microbiome and metabolome [8]. The input to MiMeNet is the relative abundances of microbial taxa, capturing the microbial composition, while its output is the predicted abundance of metabolite features. When the model is well-trained, it generates a list of metabolite features whose abundance can be well-predicted from the microbial taxa abundance. MiMeNet also provides a post-analysis procedure to identify microbe–metabolite pairs with significant interaction scores, from which members of microbes and metabolite features with similar interaction patterns can be grouped into modules of microbes and metabolite features, respectively.

For each microbial module, the naming convention was based on the upper taxonomical level (Family) of the microbes present in each module. For each metabolite module, annotated metabolites were used as inputs for the online tool MetaboAnalyst to identify metabolite sets. The analysis employed the library of "Chemical Structures" sub-chemical class metabolite sets provided by MetaboAnalyst. The resulting metabolite sets obtained

from the tool were assigned as the module name. Finally, an interaction network was constructed between microbe and metabolite modules by linking the interacting microbe–metabolite modules following the procedure of MiMeNet.

Since the neural network model requires large samples, all three strains at the genus-level microbiome profiles were combined to train models. For the metabolomes, metabolite features exhibiting zero abundance in 90% or more of the samples were removed. Following these steps, the dataset was preprocessed, resulting in a set of 91 genus-level taxa and a set of 7428 metabolite features for MiMeNet model training. To ensure the robustness of the predictions, a 10-fold cross-validation procedure was implemented in network model training. The data were randomly shuffled to create a null distribution of correlations between the predicted and observed metabolites to evaluate the significance of the prediction following the procedures of MiMeNet (https://github.com/YDaiLab/MiMeNet). The MiMeNet model was trained with the following parameters: a batch size of 1024, a learning rate of 0.001, L1 regularization of 0, L2 regularization of 0.0001, two layers with 512 nodes each, and a dropout rate of 0.5.

3. Results

The results were organized on an online server as a database website MOMMI-MP (Supplementary Figure 1A). The website's home screen has a visual representation of the basic structure of the database. Users can also explore the results of individual data types by clicking the menu bar at the top of the website. The "Structure" connects to a page that presents the flowchart of analysis performed in the database (Supplementary Figure 1B). Other tabs, such as "Metabolic Profiles," "Microbiome," and "Metabolome," include links to the respective analysis results. Here, we describe major findings included in MOMMI-MP.

3.1. Changes in metabolic profiles

Subcutaneous fat in grams tends to increase over pregnancy, especially at G15 and G19, and decreases back to baseline after pregnancy (PP3 and PP20) for the three mouse strains (Figure 2A–C). The details of other metabolic features can be accessed at "Metabolic Profiles" on the MOMMI-MP website.

3.2. Changes in microbiome

Alpha diversity over all strains exhibits an increase over the course of pregnancy through PP20 (Figure 3A). By individual mouse strain, this increasing trend holds with only outliers after the birth at PP3 for C57BL/6J and CD1 and recovers to levels from G20 by PP20 (Figure 3B–D). During pregnancy and

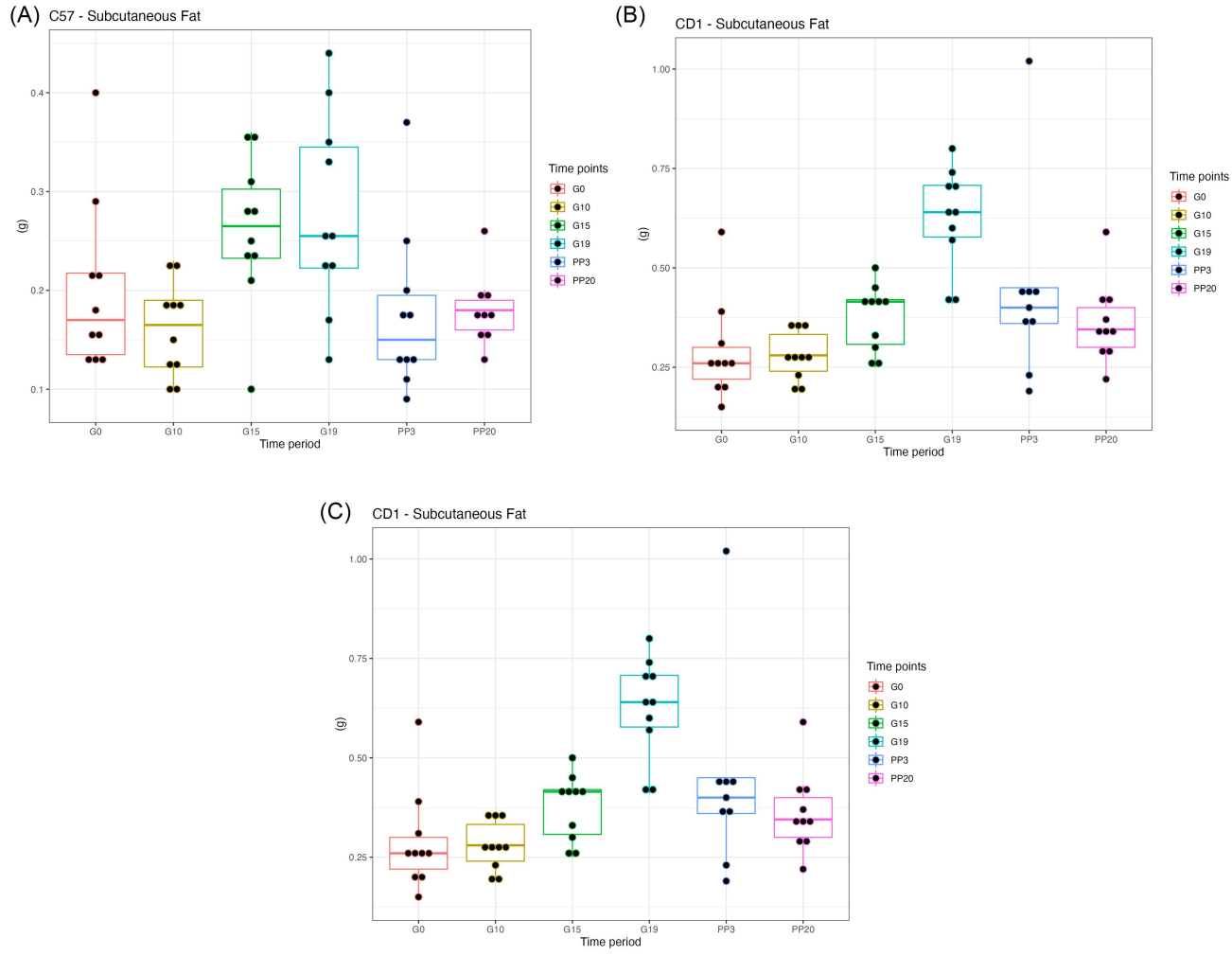

Figure 2 Metabolic profiles. The plots represent the variation in subcutaneous fat (one of the mouse health characteristics) in all three strains. (A) C57BL/6J; (B) CD1; (C) NIH-Swiss

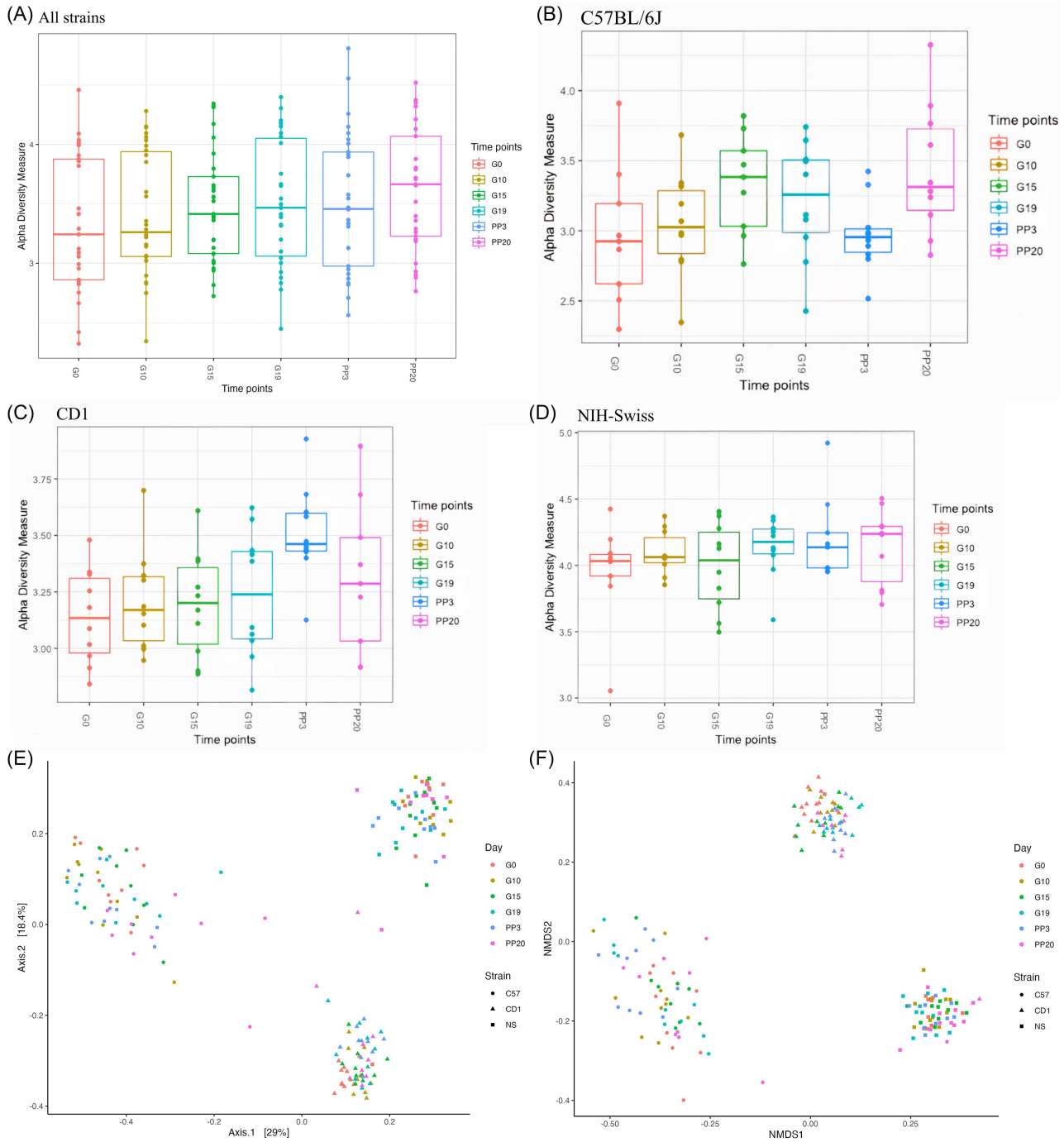

Figure 3 Alpha (Shannon) diversity. (D) All Strains; (E) C57BL/6J; (F) CD1; (G) NIH-Swiss. Beta diversity. (H) PCoA (all strains); (I) NMDS (all strains)

postpartum, Beta diversity is significantly different between mouse strains (Figure 3E–F). The microbiome composition was different between mouse strains, with Bacteriodota, Clostridia, and Bacilli comprising the majority of taxonomic classes in C57BL/6J (Supplementary Figure 2A–C).

The ANCOM-BC analysis identified DA taxa at each taxonomic level of Class, Order, Family, Genus, and Species (Table 1). For each mouse strain, there are unique DA taxa. For example, Clostridium in C57BL/6J at the Genus level (Figure 4A) and Coriobacteriaceae in C57BL/6J at the Family level (Figure 4B) increase in abundance at G15, G19, and PP3 but decrease back to baseline at PP20. Prevotella in NIH-Swiss at the Genus level decreases at G15 and G19 and increases again in PP3 (Figure 4C).

On the MOMMI-MP website, the "Microbiome" tab provides the results of differential analysis for all taxa. A table of the adjusted *p*-values can be viewed for the detected DA microbes from another linked webpage. Users can interact with the table by sorting it or searching for any specific microbe. Each microbe in the table is linked to the respective boxplots of abundance as shown in Figure 4. The webpage also provides a link redirecting the users to another webpage with results of correlation analyses of microbe–microbe, microbe–metabolic health characteristics, and microbe–metabolite, which are described later.

Table 1 The number of DA taxa obtained from ANCOM-BC for each rank in each strain

	Class	Order	Family	Genus	Species
C57BL/6J	9	10	14	6	6
CD1	8	10	17	5	7
NIH-Swiss	4	6	8	6	8

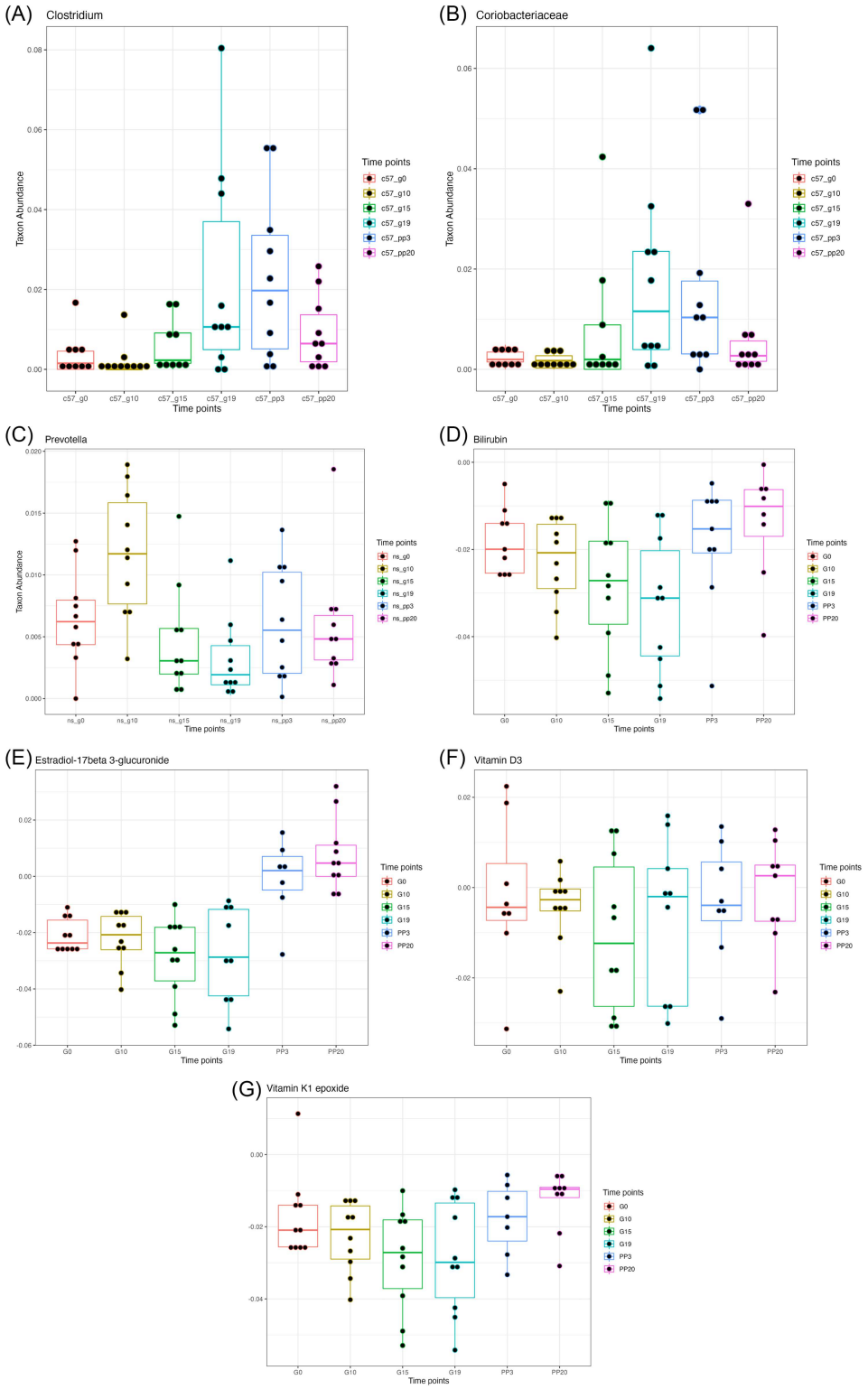

Figure 4 Examples of differentially abundant microbes. (A) Clostridium (C57BL/6J – Genus level); (B) Coriobacteriaceae (C57BL/6J – Family level); (C) Prevotella (NIH-Swiss – Genus level). Differentially abundant compounds. (D) Bilirubin; (C57BL/6J) (E) Estradiol-17β-3-glucuronide; (C57BL/6J) (F) Vitamin D3; (NIH-Swiss) (G) Vitamin K1 epoxide (C57BL/6J)

3.3. Changes in metabolites and pathway prediction

The webpage "Metabolome" provides results from the metabolome data analysis. The NMDS plots using the metabolite features after preprocessing indicate that the mice were grouped according to gestational stages, a pattern not observed in the microbiomes (Supplementary Figure 3). Since mouse models demonstrate changes to the gut microbiome and metabolome at G15 and G19 linked to insulin resistance and GDM [5], DA metabolites were initially assessed over pregnancy and postpartum. Bilirubin, estradiol-17β 3-glucuronide, vitamin D3, and vitamin K1 epoxide were identified as key metabolites that change over pregnancy and postpartum in these strains (Figure 4). Bilirubin, estradiol-17β 3-glucuronide, and vitamin K1 epoxide decreased over pregnancy, increasing to baseline in PP3 and PP20 (Figure 4D–F). The variance of vitamin D3 levels increased at G15 and G19, decreasing to baseline at PP3 and PP20 (Figure 4G). The patterns of DA metabolite features identified from the PERMANOVA analysis can be viewed on the webpage "Heatmap" (Supplementary Figure 4). These plots suggest that the differential analysis for metabolome data can be performed between G15/G19 and the rest of the time points. Further, the database can be used to investigate key microbial and metabolic changes associated with GDM.

Pathway analysis allowed us to gain insights into the biological significance and functional implications of the identified compounds within the context of pregnancy and GDM. It enables us to move beyond individual compound identification and explore how these compounds may be interconnected within specific biological processes or metabolic pathways. Using the procedures described in the Methods, we obtained the KEGG pathways significantly enriched for the DA metabolite features and the compounds identified for each strain. In our C57BL/6J mouse model, involvement of the tryptophan metabolism pathway and L-tryptophan in GDM has been indicated (Figure 5A–B) [5]. The detailed results can be viewed by clicking the "Metabolome"

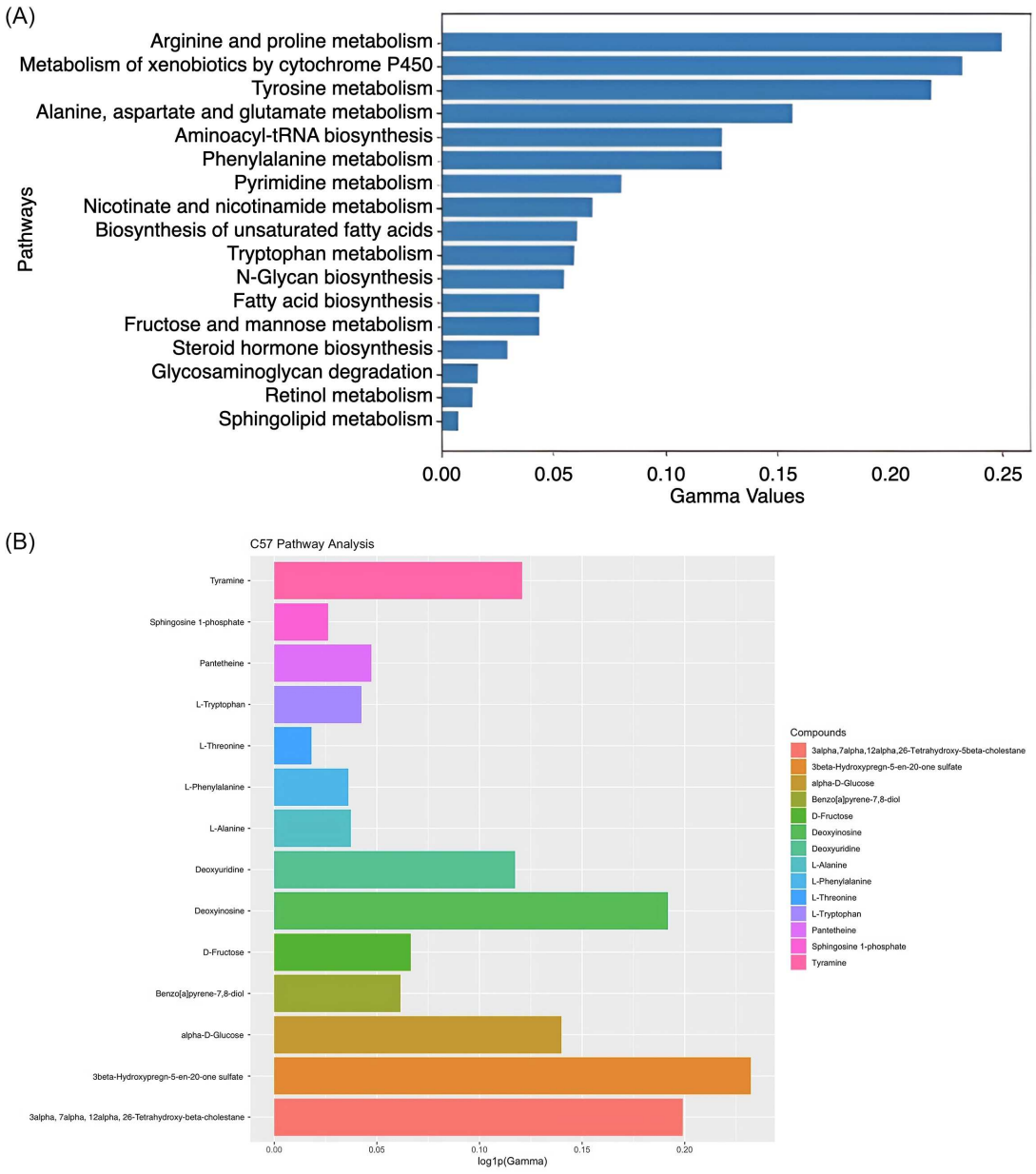

Figure 5 Pathway analysis for C57BL/6J. (A) Enriched pathways and (B) the metabolites and their gamma values obtained from the Mummichog algorithm

Table 2 Number of differentially abundant metabolite features

Strain	# Features	# Features mapped to known compounds
C57BL/6J	4784	837
CD1	3340	645
NIH-Swiss	3137	529

tab at the MOMMI-MP website. Overall, the total number of significant metabolite features and the mapped compounds for all strains are summarized in Table 2. All DA compound names can be viewed under the "Differential Abundance Analysis" tab. Users can interact with the table by sorting or searching for any specific compound name and clicking a compound name to view the respective boxplots of the abundance over the time points, as shown in Figure 4. The details of pathway analysis can be viewed under the "Pathway Analysis" tab.

3.4. Correlation of metabolites and microbes

In MOMMI-MP, the results of univariate correlation analysis were provided as follows: (1) correlations between pairs of metabolic health characteristics, (2) correlations between pairs of DA microbes and metabolic health characteristics, (3) correlations between pairs of the DA microbes, and (4) correlations between pairs of DA metabolites, and (5) correlations between pairs of the DA microbes and DA metabolites. These analyses aim to uncover microbes and metabolites associated with metabolic health characteristics (e.g., insulin resistance) during pregnancy. The analysis can also reveal the potential co-occurrence of microbial taxa that may have a mutually beneficial or competitive relationship and interactions during pregnancy and association with GDM (Figure 6A–C). The detailed correlation coefficients at each taxonomic level for each strain can be viewed by clicking the corresponding tab of "Metabolic Characteristics," "Microbiome," and "Metabolome" at the MOMMI-MP website.

3.5. Integrative analysis using MiMeNet

The objective of using MiMeNet is to unravel the intricate interplay between the gut microbiome and metabolites that are undetectable from the univariate correlation analysis. Employing the 10-fold cross-validation procedure, we first trained a robust predictive model for metabolite abundances. The model-generated performance, indicating the correlation between the predicted and observed metabolites, was 0.317, which is comparable to the results reported in the original MiMeNet paper [8]. At FDR of 0.05, we identified 88 well-predicted metabolites; the top 20 metabolites are shown in Figure 6D. All the microbes and well-predicted metabolites per module are listed in Tables 3 and 4, respectively.

To generate a holistic view of the interrelationships between microbes and metabolites, we clustered microbes and metabolites into modules using interaction scores (Figure 6E) and plotted a bipartite graph connecting microbe modules and metabolite modules with absolute average interaction scores greater than 0.3 and less than −0.3 (Figure 6F). The edges could be either negative or positive. A negative interaction indicates that the average abundance of the microbes in a module was inversely related to the average abundance of a metabolite module. Conversely, a positive interaction suggests that the average abundance of a microbe module is positively associated with the average abundance of a metabolite module. The visualization shows at the module level the complex network of interactions between the gut microbiome and metabolites during pregnancy.

In the MOMMI-MP database, an in-depth table was created to showcase the interactions of pairs of microbes and metabolites connected in the module interaction network and the microbes and metabolites that are differentially abundant, for at least one mouse strain during the pregnancy (Supplementary Figure 5). This table displays the score between each microbe and metabolite, allowing for a detailed examination of their relationships. Furthermore, the table includes the adjusted *p*-values for the DA microbes and metabolites, highlighting their relevance to pregnancy. To aid interpretation, the microbes and metabolites were denoted with upward and downward arrows at each pregnancy timepoint, representing the change in their abundance compared to the initial time point, G0 (Supplementary Figure 6). From these tables, the user can explore dynamic changes in the individual microbes and metabolites during pregnancy and their potential relevance to insulin resistance. The predicted interacting modules of microbes and metabolites from the MiMeNet analysis can be accessed at the "Integrative Analysis" tab at the MOMMI-MP website.

4. Discussion

We have developed the MOMMI-MP database to host the results of comprehensive analyses of microbiome and metabolomics time course data observed at 6 time points—gestational days 0, 10, 15, and 19 and postpartum days 3 and 20—from three mouse strains. MOMMI-MP provides results ranging from standard statistical analyses, such as differential abundance and correlation analyses, to integrative analysis of microbiome and metabolome using MiMeNet, a neural network model. The module-based integrative analysis from MiMeNet revealed potential novel relationships between microbes and metabolites during GDM.

Key metabolites that changed by gestational phase across strains included bilirubin, vitamin K, vitamin D3, and estradiol-17β 3-glucuronide. Lower bilirubin levels were observed in C57BL/6J at G15 and G19, the time points associated with heightened insulin resistance in mouse pregnancy (Figure 4D). Historically known as a waste product, bilirubin has only recently been recognized as a potent antioxidant, immunosuppressant, and metabolic hormone affecting cell signaling [19]. Lower bilirubin levels are associated with metabolic dysfunction, obesity, and inflammation [20]. How bilirubin affects the physiological state of pregnancy is unknown. Few correlational studies show hypobilirubinemia to be associated with an increased risk of GDM in humans [21–24]. Levels of vitamin K were observed to be reduced during the insulin resistance phase of mouse pregnancy (at one or both of the time points, G15 and G19) and increased during the postpartum period (PP3 and PP20) (Figure 4G). Vitamin K supplementation has been suggested to lower the risk of developing diabetes, possibly through improving insulin sensitivity [25, 26]. Estradiol-17β 3-glucuronide was found relatively lower at G15 and G19 and higher at PP3 and PP20 in C57BL/6J and

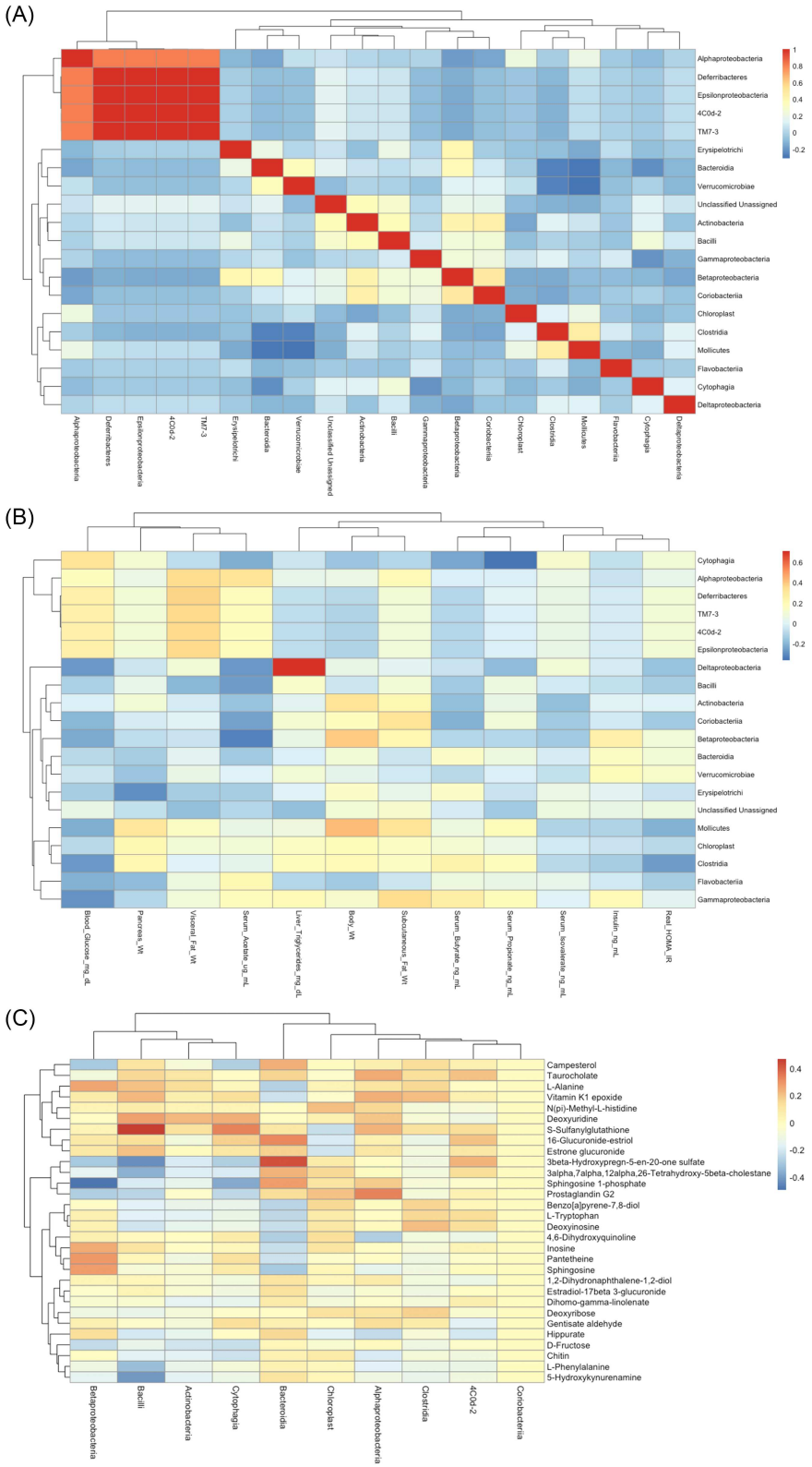

NIH-Swiss mice (Figure 4E). Of relevance, estradiol-17β 3-glucuronide is thought to stabilize and prevent deterioration of the metabolic state of prediabetic mice via increasing glucose-stimulated insulin secretion and improving hepatic glucose utilization [27, 28].

Other metabolites are identified as significant through modules with significant microbes in the network analysis including lipid metabolism in Module 1 (Figure 6). Lipid metabolism changes significantly during pregnancy, and its disruption is associated with GDM [29–31]. The modules of microbes and metabolites from our analysis may provide additional insights into their relationship to metabolic alterations during pregnancy.

The microbe and metabolite interplay (Supplementary Figures 5 and 6) is interconnected in the module interaction

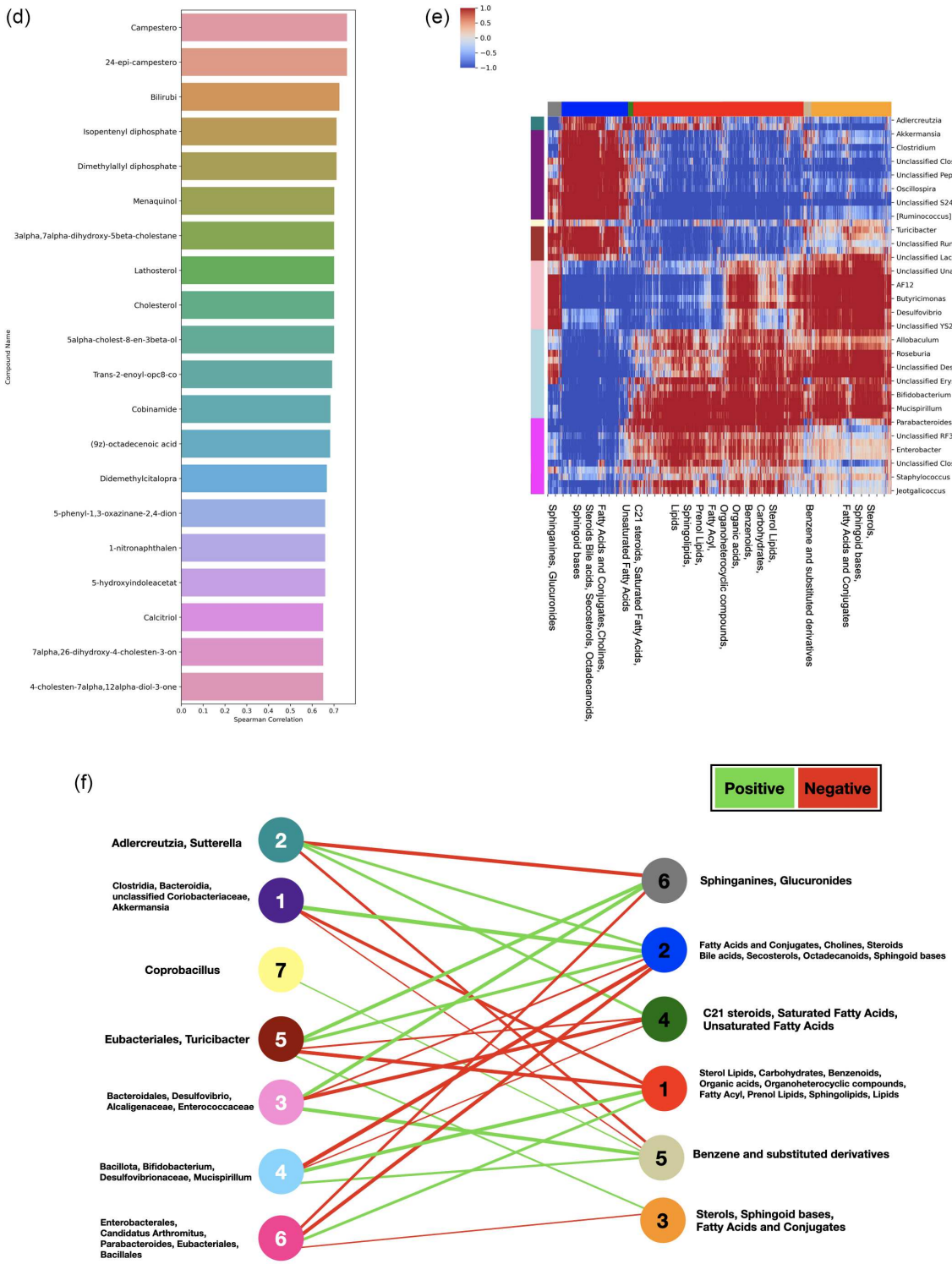

Figure 6 Results of correlation analysis for C57BL/6J. (A) correlations between microbe–microbe pairs (class level); (B) correlations between microbe (class level)–metabolic characteristic pairs; (C) correlations between metabolite–microbe pairs. Prediction of metabolites' abundance from MiMeNet. (D) The top 20 predicted metabolites. (E) Clustering of microbes (row) and metabolites (column) based on the feature attribution scores. Row and column colors represent assigned modules. (F) Network connecting microbial modules with metabolomic modules. The name of each microbe module indicates the microbes' upper taxonomical level, and the name of each metabolite module indicates the metabolite set obtained from the Mummichog algorithm. The colors represent different modules for microbes and metabolites. Red edges represent negative interaction, and green edges represent positive interaction. The width of the edges represents the strength of the interaction. Thin edges represent low interaction, and wide edges represent strong interaction

Table 3 Microbes per module

Microbes	Module
Akkermansia	1
Anaerostipes	
Bacteroides	
Clostridium	
Unclassified Coriobacteriaceae	
Unclassified Peptostreptococcaceae	
[Prevotella]	
Adlercreutzia	2
Odoribacter	3
Prevotella	
Unclassified Bacteroidales	
Bifidobacterium	4
Lactobacillus	
Roseburia	
Unclassified Rikenellaceae	
Anaeroplasma	5
Turicibacter	
Candidatus Arthromitus	6
Corynebacterium	
Jeotgalicoccus	
Parabacteroides	
Staphylococcus	
Unclassified Enterobacteriaceae	
Unclassified mitochondria	
rc4-4	

network (Figure 6), providing additional insights. Interestingly, several interactions were observed between bilirubin and specific gut microbial genera (Figure 6). Coriobacteriaceae and Clostridium interacted negatively with bilirubin and were highly abundant at G19 and PP3 (Figure 4B). Clostridium has been shown to reduce bilirubin [20], and members of the Coriobacteriaceae family facilitate important metabolic functions in the conversion of bile acids, steroids, or phytoestrogens [24]. Similar interactions were noted with several gut bacteria for fat-soluble vitamins: vitamin K in C57BL/6J and vitamin D in NIH-Swiss. The gut microbiome is a primary source of vitamin K [26]. Clostridium (Module 1) interacts negatively with vitamin K and was found to be higher at G19 and PP3 (Figure 4A). Members of Clostridiales cannot synthesize vitamin K and flourish under micronutrient deficiency [26]. Further, persistent *Clostridium difficile* infection has been shown to be associated with vitamin K deficiency. Thus, the role of this increased abundance as a consequence or contributor to altered metabolism in pregnancy needs research. It has also been suggested that vitamin D deficiency is a potential risk factor for *Clostridium difficile* infection [32], and the administration of vitamin D (calcitriol) may enhance insulin sensitivity and improve glucose tolerance during pregnancy [33]. Staphylococcus (Module 6) interacts negatively with estradiol-17β 3-glucuronide; however, its abundance levels do not show significant changes in our data. Another taxon with positive interaction with estradiol-17β 3-glucuronide is Prevotella (Module 3). Its abundance in NIH-Swiss mice was found to be significantly reduced after G15 (Figure 4C). Prevotella is involved in a wide range of functions through its main fermentation byproduct propionate [34]. However, there is no documented research on the relationship between Prevotella and estradiol-17β 3-glucuronide. Whether these interactions are meaningful in the context of pregnancy, and if these are the cause or consequence of pregnancy-insulin resistance, requires experimental validation. Nonetheless, these findings from the literature imply the potential of MOMMI-MP to generate novel hypotheses related to mechanisms underlying metabolic alterations during pregnancy.

No currently available dedicated databases report a comprehensive analysis from well-designed multi-omics studies during human or mouse pregnancy. The Vaginal Microbiome Consortium conducted the Multi-Omic Microbiome Study: Pregnancy Initiative (MOMS-PI) to better understand the dynamics of vaginal microbiome and host profiles during pregnancy and the establishment of the nascent microbiome in neonates, with samples collected from 1594 women and their neonates throughout pregnancy, at delivery, and postpartum. However, no comprehensive platform analysis of the results was provided. Another database, iMOMdb, provides the first blood-based multi-omics analysis of Asian pregnant women [35]. It collected high-resolution genotyping ($N = 1079$), DNA methylation ($N = 915$), and transcriptome profiling ($N = 238$). The integrative omics analysis presented in iMOMdb identified pathways involved in lipid metabolism, the adaptive immune system, and carbohydrate metabolism through ethnicity-specific quantitative traits hotspots, indicating significant lipid differences among Chinese, Malay, and Indian women. Nonetheless, we should note that our database may be limited in its power to detect more subtle effects, as we have a smaller sample size. Further, our study focused on mouse

Table 4 Well-predicted metabolites per module

Metabolites	Modules	Metabolites	Modules
1-Nitro-5,6-dihydroxy-dihydronaphthalene	1	L-Cysteate	1
11β,17α,21-Trihydroxypregnenolon		L-Glutamate 5-semialdehyde	
11β,21-Dihydroxy-3,20-oxo-5β-pregnan-18-a		L-Metanephrin	
11β-Hydroxyprogesterone		L-Palmitoylcarnitin	
1a,11b-Dihydro-4,9-dimethylbenz[a]anthra[3,4-b]oxiren		Leukotriene A4	
20α-Hydroxy-4-pregnen-3-one		Octadecanoic acid	
20α-Hydroxycholesterol		Pregnenolone	
22(R)-Hydroxycholesterol		S-Adenosyl-L-homocysteine	
24-epi-Campestero		Sphingosine	
25-Hydroxycholesterol		Testosterone glucuronide	
3-Dehydrosphinganine		Vitamin K1 epoxide	
3α,7α,12α-Trihydroxy-5β-cholestan-26-a		Xylito	
3α,7α,12α-Trihydroxy-5β-cholestane		cis-4-Hydroxy-D-prolin	
3α,7α,26-Trihydroxy-5β-cholestane		trans-3-Hydroxy-L-proline	
3α,7α-Dihydroxy-5β-cholestanate	1	(24S)-Cholest-5-ene-3β,7α,24-triol	2
3β-Hydroxy-5-cholestenoate		1-Nitronaphthalen	
4-(2-Aminophenyl)-2,4-dioxobutanoat		17α,20α-Dihydroxycholestero	
4-Cholesten-7α,12α-diol-3-one		20α,22β-Dihydroxycholesterol	
5-Amino-2-oxopentanoic acid		3-Carbamoyl-2-phenylpropionaldehyd	
5-Aminolevulinate		3α,7α-Dihydroxy-5β-cholestan-26-a	
5α-Pregnane-3,20-dione		3β,7α-Dihydroxy-5-cholestenoate	
5β-Pregnane-3,20-dion		4-Hydroxy-5-phenyltetrahydro-1,3-oxazin-2-on	
7,12-Dimethylbenz[a]anthracene		5-Hydroxy-L-tryptophan	
7,12-Dimethylbenz[a]anthracene 5,6-oxide		5-Hydroxyindoleacetat	
7-Hydroxymethyl-12-methylbenz[a]anthracene		5-Phenyl-1,3-oxazinane-2,4-dion	
7α,24-Dihydroxy-4-cholesten-3-on		5α-Cholesta-7,24-dien-3β-o	
7α,25-Dihydroxy-4-cholesten-3-on		5α-Pregnan-20α-ol-3-one	
7α,27-Dihydroxycholesterol		7-Dehydrocholesterol	
7α-Hydroxy-5β-cholestan-3-one		7α,12α-Dihydroxy-5β-cholestan-3-one	
7α-Hydroxycholesterol		7α,26-Dihydroxy-4-cholesten-3-on	
Benzo[a]pyrene		7α-Hydroxycholest-4-en-3-on	
Bilirubin	1	Allopregnanolone	2
Calcitriol		Calcidiol	
Campestero		Calcitetrol	
Cerebrosterol		Desmosterol	
Cholest-5-ene-3β,26-diol		Linoleate	
Cholest-5-ene-3β,7α,25-triol		Phenylacetylglycin	
Cholic acid		Secalciferol	
Didemethylcitalopra		Vitamin D3	
Dihydrocortisol		Zymosterol	2
Dimethylallyl diphosphate		(5Z,8Z,11Z,14Z,17Z)-Icosapentaenoic acid	4
Hydroxyproline		2-Phenyl-1,3-propanediol monocarbamate	5
Isopentenyl diphosphate		5-Fluorouridin	6
L-Arabitol		Estradiol-17β 3-glucuronide	

samples. For example, in our recent publication, we have used these data to identify that kynurenine has a role in metabolic changes during pregnancy, and in this report, we have used human fecal samples to translate these effects [5]. In contrast, our database, MOMMI-MP, is the first to provide a comprehensive analysis of physiological and metabolic responses, gut microbiome, and plasma metabolome from our three mouse strains during pregnancy.

5. Conclusion

The MOMMI-MP database provides comprehensive analysis results of the metabolic health characteristics, microbiome, and metabolome data obtained from three genetically distinct strains of mice (C57BL/6J, CD1, and NIH-Swiss) during the gestational and postpartum stages. In a form accessible to researchers with limited access to bioinformatics tools, MOMMI-MP is an easy-to-use platform that enables exploration of the results of the analysis. MOMMI-MP may facilitate the identification of novel metabolite- or microbiome-based therapeutic targets to mitigate the risk of developing type 2 diabetes later in life.

Acknowledgment

BTL acknowledges support from NIH R01DK104927-01A1, NIH P30DK020595, and VA merit 1I01BX003382-01-A1. The funders had no roles in study design, data collection and analysis, decision to publish, or manuscript preparation.

Ethical Statement

This study did not generate new animal data. All animal data analyzed in this paper were obtained from a previously published study by Priyadarshini et al. [5]. All animal experiments reported in the original publication were conducted in accordance with relevant institutional and national guidelines and were approved by the appropriate ethics committee, with the corresponding ethical approval numbers fully reported in the original article.

Conflicts of Interest

The authors declare that they have no conflicts of interest to this work.

Data Availability Statement

The data that support the findings of this study are openly available in the MOMMI-MP database at https://mommi-mp.github.io/Plots/index.html.

Author Contribution Statement

Kaustubh K. Pachpor: Methodology, Software, Validation, Formal analysis, Investigation, Resources, Data curation, Writing – original draft, Visualization. **Julianne Jorgensen:** Methodology, Formal analysis, Investigation, Resources, Data curation, Writing – review & editing, Visualization. **Medha Priyadarshini:** Methodology, Validation, Formal analysis, Investigation, Resources, Data curation. **Derek J. Reiman:** Methodology, Formal analysis, Investigation, Resources, Data curation. **Brian T. Layden:** Conceptualization, Investigation, Resources, Writing – review & editing, Supervision, Project administration. **Yang Dai:** Conceptualization, Methodology, Software, Investigation, Resources, Data curation, Writing – review & editing, Supervision, Project administration.

Supplementary material

The supplementary material for this article can be found at https://doi.org/10.47852/bonviewMEDIN52027245

References

[1] Gregory, E. C., & Ely, D. M. (2022). Trends and characteristics in gestational diabetes: United States, 2016–2020. *National Vital Statistics Reports*, *71*(3), 1–15. https://doi.org/10.15620/cdc:118018

[2] Centers for Disease Control and Prevention. (2023). QuickStats: Percentage of mothers with gestational diabetes,* by maternal age – National Vital Statistics System, United States, 2016 and 2021. *MMWR. Morbidity and Mortality Weekly Report*, *72*(1), 16. https://doi.org/10.15585/mmwr.mm7201a4

[3] Angueira, A. R., Ludvik, A. E., Reddy, T. E., Wicksteed, B., Lowe Jr, W. L., & Layden, B. T. (2015). New insights into gestational glucose metabolism: lessons learned from 21st century approaches. *Diabetes*, *64*(2), 327–334. https://doi.org/10.2337/db14-0877

[4] Sonagra, A. D., Biradar, S. M., & DS, J. M. (2014). Normal pregnancy-a state of insulin resistance. *Journal of Clinical and Diagnostic Research: JCDR*, *8*(11), CC01. https://doi.org/10.7860/JCDR/2014/10068.5081

[5] Priyadarshini, M., Navarro, G., Reiman, D. J., Sharma, A., Xu, K., Lednovich, K., . . . , & Layden, B. T. (2022). Gestational insulin resistance is mediated by the gut microbiome–indoleamine 2, 3-dioxygenase axis. *Gastroenterology*, *162*(6), 1675–1689. https://doi.org/10.1053/j.gastro.2022.01.008

[6] Wang, S., Liu, Y., Tam, W. H., Ching, J. Y., Xu, W., Yan, S., . . . , & Zhang, L. (2024). Maternal gestational diabetes mellitus associates with altered gut microbiome composition and head circumference abnormalities in male offspring. *Cell Host & Microbe*, *32*(7), 1192–1206. https://doi.org/10.1016/j.chom.2024.06.005

[7] Spor, A., Koren, O., & Ley, R. (2011). Unravelling the effects of the environment and host genotype on the gut microbiome. *Nature Reviews Microbiology*, *9*(4), 279–290. https://doi.org/10.1038/nrmicro2540

[8] Reiman, D., Layden, B. T., & Dai, Y. (2021). MiMeNet: Exploring microbiome-metabolome relationships using neural networks. *PLoS Computational Biology*, *17*(5), e1009021. https://doi.org/10.1371/journal.pcbi.1009021

[9] Reutrakul, S., Chen, H., Chirakalwasan, N., Charoensri, S., Wanitcharoenkul, E., Amnakkittikul, S., . . . , & Chlipala, G. E. (2021). Metabolomic profile associated with obstructive sleep apnoea severity in obese pregnant women with gestational diabetes mellitus: A pilot study. *Journal of Sleep Research*, *30*(5), e13327. https://doi.org/10.1111/jsr.13327

[10] Röst, H. L., Sachsenberg, T., Aiche, S., Bielow, C., Weisser, H., Aicheler, F., . . . , & Kohlbacher, O. (2016). OpenMS: a flexible open-source software platform for mass spectrometry data analysis. *Nature Methods*, *13*(9), 741–748. https://doi.org/10.1038/nmeth.3959

[11] Wishart, D. S., Feunang, Y. D., Marcu, A., Guo, A. C., Liang, K., Vázquez-Fresno, R., . . . , & Scalbert, A. (2018). HMDB 4.0: The human metabolome database for 2018.

Nucleic Acids Research, *46*(D1), D608–D617. https://doi.org/10.1093/nar/gkx1089

[12] Caporaso, J. G., Kuczynski, J., Stombaugh, J., Bittinger, K., Bushman, F. D., Costello, E. K., . . . , & Knight, R. (2010). QIIME allows analysis of high-throughput community sequencing data. *Nature Methods*, *7*(5), 335–336. https://doi.org/10.1038/nmeth.f.303

[13] McMurdie, P. J., & Holmes, S. (2013). phyloseq: An R package for reproducible interactive analysis and graphics of microbiome census data. *PloS One*, *8*(4), e61217. https://doi.org/10.1371/journal.pone.0061217

[14] Oksanen, J., Simpson, G., Blanchet, F., Kindt, R., Legendre, P., Minchin, P., & Weedon, J. (2025). Vegan: Community Ecology Package. R package version 2.7-0. https://doi.org/10.32614/CRAN.package.vegan

[15] Lin, H., & Peddada, S. D. (2020). Analysis of compositions of microbiomes with bias correction. *Nature Communications*, *11*(1), 3514. https://doi.org/10.1038/s41467-020-17041-7

[16] Anderson, M. J. (2014). Permutational multivariate analysis of variance (PERMANOVA). Wiley statsref: Statistics reference online. 1–15. https://doi.org/10.1002/9781118445112.stat07841

[17] Pang, Z., Zhou, G., Ewald, J., Chang, L., Hacariz, O., Basu, N., & Xia, J. (2022). Using MetaboAnalyst 5.0 for LC–HRMS spectra processing, multi-omics integration and covariate adjustment of global metabolomics data. *Nature Protocols*, *17*(8), 1735–1761. https://doi.org/10.1038/s41596-022-00710-w

[18] Tenenbaum, D., & Maintainer, B. (2025). *KEGGREST: Client-side REST access to the Kyoto Encyclopedia of Genes and Genomes (KEGG). R package version 1.50.0*. https://doi.org/10.18129/B9.bioc.KEGGREST

[19] Vitek, L., Hinds, T. D., Stec, D. E., & Tiribelli, C. (2023). The physiology of bilirubin: Health and disease equilibrium. *Trends in Molecular Medicine*, *29*(4), 315–328. https://doi.org/10.1016/j.molmed.2023.01.007

[20] Creeden, J. F., Gordon, D. M., Stec, D. E., & Hinds Jr, T. D. (2021). Bilirubin as a metabolic hormone: The physiological relevance of low levels. *American Journal of Physiology-Endocrinology and Metabolism*, *320*(2), E191–E207. https://doi.org/10.1152/ajpendo.00405.2020

[21] Nishimura, T., Tanaka, M., Saisho, Y., Miyakoshi, K., Tanaka, M., & Itoh, H. (2018). Lower serum total bilirubin concentration is associated with higher prevalence of gestational diabetes mellitus in Japanese pregnant women. *Endocrine Journal*, *65*(12), 1199–1208. https://doi.org/10.1507/endocrj.EJ17-0533

[22] Liu, C., Zhong, C., Zhou, X., Chen, R., Wu, J., Wang, W., . . . , & Yang, N. (2017). Higher direct bilirubin levels during mid-pregnancy are associated with lower risk of gestational diabetes mellitus. *Endocrine*, *55*(1), 165–172. https://doi.org/10.1007/s12020-016-1103-6

[23] He, W., Wang, L., Zhang, Y., Jiang, Y., Chen, X., Wang, Y., . . . , & Yan, W. (2021). Higher serum bilirubin levels in response to higher carbohydrate intake during early pregnancy and lower gestational diabetes mellitus occurrence in overweight and obese gravidae. *Frontiers in Nutrition*, *8*, 701422. https://doi.org/10.3389/fnut.2021.701422

[24] Ridlon, J. M., Kang, D. J., Hylemon, P. B., & Bajaj, J. S. (2014). Bile acids and the gut microbiome. *Current Opinion in Gastroenterology*, *30*(3), 332–338. https://doi.org/10.1097/MOG.0000000000000057

[25] Ho, H. J., Komai, M., & Shirakawa, H. (2020). Beneficial effects of vitamin K status on glycemic regulation and diabetes mellitus: A mini-review. *Nutrients*, *12*(8), 2485. https://doi.org/10.3390/nu12082485

[26] Ellis, J. L., Karl, J. P., Oliverio, A. M., Fu, X., Soares, J. W., Wolfe, B. E., . . . , & Booth, S. L. (2021). Dietary vitamin K is remodeled by gut microbiota and influences community composition. *Gut Microbes*, *13*(1), 1887721. https://doi.org/10.1080/19490976.2021.1887721

[27] Kang, M. J., Baek, K. R., Lee, Y. R., Kim, G. H., & Seo, S. O. (2022). Production of vitamin K by wild-type and engineered microorganisms. *Microorganisms*, *10*(3), 554. https://doi.org/10.3390/microorganisms10030554

[28] Liebmann, M., Asuaje Pfeifer, M., Grupe, K., & Scherneck, S. (2022). Estradiol (E2) improves glucose-stimulated insulin secretion and stabilizes GDM progression in a prediabetic mouse model. *International Journal of Molecular Sciences*, *23*(12), 6693. https://doi.org/10.3390/ijms23126693

[29] Zhan, Y., Wang, J., He, X., Huang, M., Yang, X., He, L., . . . , & Lou, Y. (2021). Plasma metabolites, especially lipid metabolites, are altered in pregnant women with gestational diabetes mellitus. *Clinica Chimica Acta*, *517*, 139–148. https://doi.org/10.1016/j.cca.2021.02.023

[30] Liang, L., Rasmussen, M. L. H., Piening, B., Shen, X., Chen, S., Röst, H., . . . , & Melbye, M. (2020). Metabolic dynamics and prediction of gestational age and time to delivery in pregnant women. *Cell*, *181*(7), 1680–1692. https://doi.org/10.1016/j.cell.2020.05.002

[31] Ogundipe, E., Samuelson, S., & Crawford, M. A. (2020). Gestational diabetes mellitus prediction? A unique fatty acid profile study. *Nutrition & Diabetes*, *10*(1), 36. https://doi.org/10.1038/s41387-020-00138-9

[32] Youssef, D., Grant, W. B., & Peiris, A. N. (2012). Vitamin D deficiency: A potential risk factor for Clostridium difficile infection. *Risk Management and Healthcare Policy*, *5*, 115–116. https://doi.org/10.2147/RMHP.S36781

[33] Wong, K. K., Lee, R., Watkins, R. R., & Haller, N. (2016). Prolonged Clostridium difficile infection may be associated with vitamin D deficiency. *Journal of Parenteral and Enteral Nutrition*, *40*(5), 682–687. https://doi.org/10.1177/0148607114568121

[34] Betancur-Murillo, C. L., Aguilar-Marín, S. B., & Jovel, J. (2022). Prevotella: A key player in ruminal metabolism. *Microorganisms*, *11*(1), 1. https://doi.org/10.3390/microorganisms11010001

[35] Pan, H., Tan, P. F., Lim, I. Y., Huan, J., Teh, A. L., Chen, L., . . . , & Karnani, N. (2022). Integrative multi-omics database (iMOMdb) of Asian pregnant women. *Human Molecular Genetics*, *31*(18), 3051–3067. https://doi.org/10.1093/hmg/ddac079

How to Cite: Pachpor, K. K., Jorgensen, J., Priyadarshini, M., Reiman, D. J., Layden, B. T., & Dai, Y. (2026). MOMMI-MP: A Comprehensive Database for Integrated Analysis of Metabolic and Microbiome Profiling of Mouse Pregnancy. *Medinformatics*. https://doi.org/10.47852/bonviewMEDIN62027245